Electron paramagnetic resonance spectroscopy of Cr^{3+} from the growth bands of potassium dihydrogen phosphate

1989 J. Phys.: Condens. Matter 1 6145

(http://iopscience.iop.org/0953-8984/1/35/013)

J. Phys.: Condens. Matter 1 (1989) 6145–6151. Printed in the UK

Electron paramagnetic resonance spectroscopy of Cr^{3+} from the growth bands of potassium dihydrogen phosphate

D Bravo†, F J López†, E Diéguez†, M Aguilar‡ and J M Cabrera†

† Departamento de Física Aplicada C-IV, Universidad Autónoma de Madrid, Cantoblanco, E-28049 Madrid, Spain

‡ Instituto de Ciencia de Materiales, Consejo Superior de Investigaciones Científicas, Universidad Autónoma de Madrid, Cantoblanco, E-28049 Madrid, Spain

Received 4 November 1988

Abstract. Samples taken from the growth band region of a KDP : Cr crystal have been studied by EPR spectroscopy at room temperature. The observed lines are consistent with a centre in which Cr^{3+} substitutes for K^+ with two proton vacancies in nearest positions. From the powder spectrum and the angular variation of the resonance fields the defect principal axes and the spin-Hamiltonian parameters have been calculated. The experimental spectra, the angular variation and the parameters obtained resemble those from samples taken from regions out of the growth bands. The differences between Cr^{3+} spectra in both types of sample are attributed to variations in the crystal-field strength produced by changes in the lattice parameters.

1. Introduction

KDP is an important electro-optic crystal because of its applications in laser beam modulators, second-harmonic generation and other practical electro-optic devices. Its phase transition has also been the subject of considerable interest from the viewpoint of basic research. In both applied and basic fields, knowledge and control of defects and impurities play an important role. In practical applications, absorption and scattering from defects and impurities have to be minimised as much as possible for optimum performance. On the contrary, impurities have often been used as convenient probes in electron paramagnetic resonance (EPR) spectroscopy to monitor the KDP phase transition (at 123 K) following the method first introduced in [1] for $SrTiO_3$. A number of paramagnetic impurities, as well as several radicals produced by x-ray, γ-ray and electron irradiation have already been investigated by EPR [2, 3] and optical spectroscopies [4–9], and their relevance in the mentioned field emphasised.

Impurity spectroscopy of KDP often presents difficulty associated with a low level of impurity concentration in the lattice, which implies handling spectra with low signal-to-noise ratios. This low concentration is mainly related to the low distribution coefficients that most impurities have at the temperature (near room temperature) at which KDP crystals are usually grown from aqueous solutions. In order to improve the signal-to-noise ratio of the spectra, samples from the so-called 'growth bands' have previously

0953-8984/89/356145 + 07 $02.50

been used [10], since they exhibit a higher impurity concentration than does the rest of the crystal. These growth band samples, however, have slightly different lattice parameters, as reported in [11], which may considerably affect their spectroscopic analysis.

In the course of a study of KDP samples from these growth bands, EPR spectra of Cr^{3+} have been found to differ from those previously reported [12]. The EPR spectra of polyvalent cations such as Cr^{3+} in KDP are known to be rich and complex because of the low local symmetry they present. Two or more H^+ (or K^+) vacancies are often involved in the process of local charge compensation, producing a considerable distortion of the positions of the surrounding ions. Since the spectra show a high sensitivity to the sample orientation, non-negligible differences may easily arise from very small misorientations. Therefore, special care must be taken in the orientation procedure in order to ascertain that the observed differences do not come from only small misorientations.

In this paper, EPR spectra of Cr^{3+} in a KDP sample taken from the growth band region will be presented together with the angular variation of the resonance fields. Particular attention will be paid to details of sample orientation, in order to overcome the problem mentioned above. It will be shown that the differences observed in spectra taken from our growth band sample are due to the occurrence of a different Cr^{3+} centre in these samples. The principal axes and the spin-Hamiltonian parameters of the new centre will be compared with those previously reported [12] in order to elucidate the physical implications of the observed differences.

2. Experimental details

A Cr-doped KDP crystal was grown in our laboratory by the temperature decrease method, i.e. by slowly cooling (from about 70 to about 40 °C) a saturated aqueous solution to which $CrCl_3$ was added. With this procedure a KDP prism tapered along the tetragonal crystallographic axis (*c* axis) was obtained with an approximate size of 15 mm × 7.5 mm × 5 mm. A prism orientation finer than that given by the natural growth faces was carried out by taking a number of Laue x-ray diffraction patterns, the estimated angular error being ±0.5°. Once the crystal was oriented and before it was taken out of the goniometer, a plate approximately 1 mm thick was sawn from a prismatic face, i.e. most of the growth band zone [10] was taken. This plate was split into two halves to be used for the angular variation measurements and the powder spectrum, respectively. This last sample was later used for atomic absorption spectrometric analysis, giving a Cr concentration of about 100 ppm.

The EPR spectra were obtained with a Varian E-12 spectrometer in the X band with a field modulation frequency of 100 kHz at room temperature. Accurate values of the resonance magnetic fields and microwave frequencies were measured with a Bruker gaussmeter (model ER 035 M) and a Hewlett–Packard frequency meter (model 5342A), respectively. The sample was placed in a home-made two-axis goniometer, so that it could be rotated in two perpendicular planes. This goniometer allowed a more accurate *in situ* sample orientation, giving excellent resonance field reproducibility on 180° rotations. The same goniometer was used to obtain the angular variation of the resonance fields.

3. Results

Figure 1 shows an EPR spectrum of a KDP:Cr sample obtained from the growth band region as mentioned above. It was obtained with $\boldsymbol{H}$ parallel to the crystallographic *c* axis.

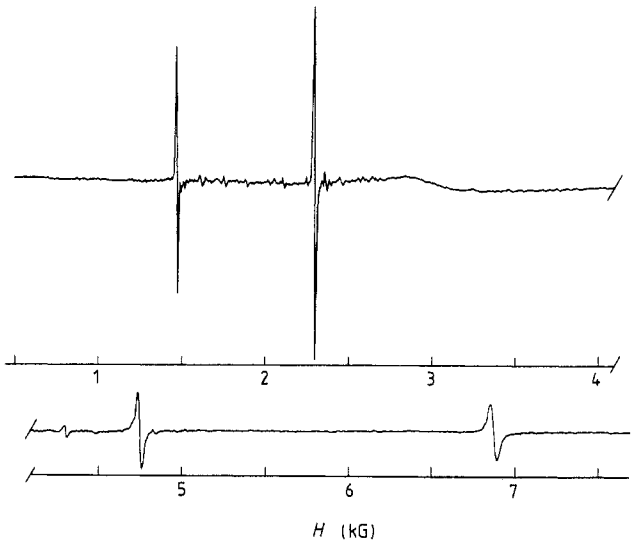

Figure 1. EPR spectrum, measured at room temperature, of a sample of KDP : Cr^{3+} taken from the growth band region of the crystal, with the external magnetic field parallel to the *c* axis.

This spectrum resembles that reported in [12] and attributed to Cr^{3+} ions that substitute for K^+, although small differences in the values of the resonance fields can be observed. Other weak bands arising from unknown defects or impurities are very small in this figure. The analysis of these bands is left until future work and they will be not further considered in the present paper. In figure 2 a full angular variation of the resonance fields is plotted for rotations around both the *c* and the *a* crystallographic axes. The open circles indicate the experimental fields measured every 2 or 3°. From this angular variation it is inferred that Cr^{3+} ions have an orthorhombic symmetry. Again, figure 2 resembles the equivalent figure reported in [12] for the Cr^{3+} ion, although the angular dependences exhibit noticeable differences which will be discussed below. Comments similar to those made for figures 1 and 2 also apply when comparing powder spectra from both studies.

It seems sensible therefore to assume that we are also dealing with Cr^{3+} ions that substitute for K^+, although the crystal-field strength somehow must be different. From the powder spectrum and the directions of maximum splitting a crude estimate of the spin-Hamiltonian parameters and the directions of the defect principal axes was obtained. As a consequence of the KDP lattice symmetry (space group, $I\bar{4}2d$), eight equivalent defects are present with the directions of their principal axes related by the point group $\bar{4}2m$. The directions of the *Z* and *Y* axes for the eight defects approximately coincide with the directions of the K^+–H^+ nearest-neighbour pairs. These directions are drawn on the KDP lattice in figure 3.

Starting from these approximate values, a more accurate determination of all of them has been achieved by fitting the resonance field values computed with the spin Hamiltonian to the experimental values shown in figure 2. The effective spin Hamiltonian for the $^4A_2$ ground state of Cr^{3+} in the defect axes system is

$$\mathcal{H} = \beta \boldsymbol{H} \cdot \hat{\boldsymbol{g}} \cdot \boldsymbol{S} + B_2^0[3S_z^2 - S(S+1)] + B_2^2[S_x^2 - S_y^2]$$

with $S = \frac{3}{2}$. In order to relate the crystallographic axes *a*, *b* and *c* to the defect principal axes *X*, *Y* and *Z*, the common Eulerian angles [12] have been used. The fitting process

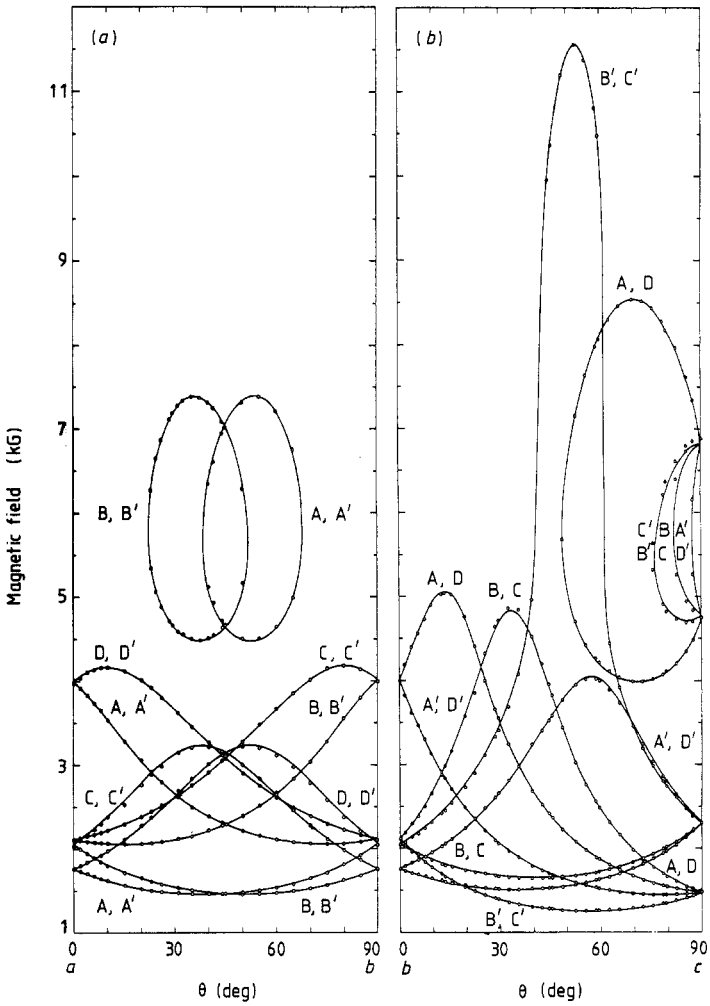

Figure 2. Angular dependence of the EPR spectrum at room temperature of KDP: Cr^{3+} (growth band region) with the magnetic field lying in the *a–b* and *b–c* planes: ○, experimental fields; ——, calculated values with the fitting parameters and angles. Each of the labels A, A′, B, B′, C, C′, D and D′ designates one set of the principal axes (see text and figure 3).

was carried out by numerical diagonalisation of the energy matrices by the Jacoby method, so that eigenvalues as well as eigenfunctions were obtained. A minimisation subroutine gave the resonance fields for each set of parameters and Eulerian angles. The resonance field values obtained whenever the fitting process is concluded are plotted as a full line in figure 2. The best set of spin-Hamiltonian parameters and Eulerian angles obtained with this fitting are included in table 1.

In figure 4 the calculated energies of the different levels are plotted as a function of the external magnetic field intensity for $\boldsymbol{H}$ parallel to the crystallographic *c* axis. Although the closed loop appearing in figure 2 is seldom observed, it is worth mentioning that this shape is correctly predicted by the computed values as shown by the full line. The reason is that the $|\frac{1}{2}\rangle \rightarrow |-\frac{1}{2}\rangle$ transition can take place at two different field values for a certain range of sample orientations, as shown in figure 4.

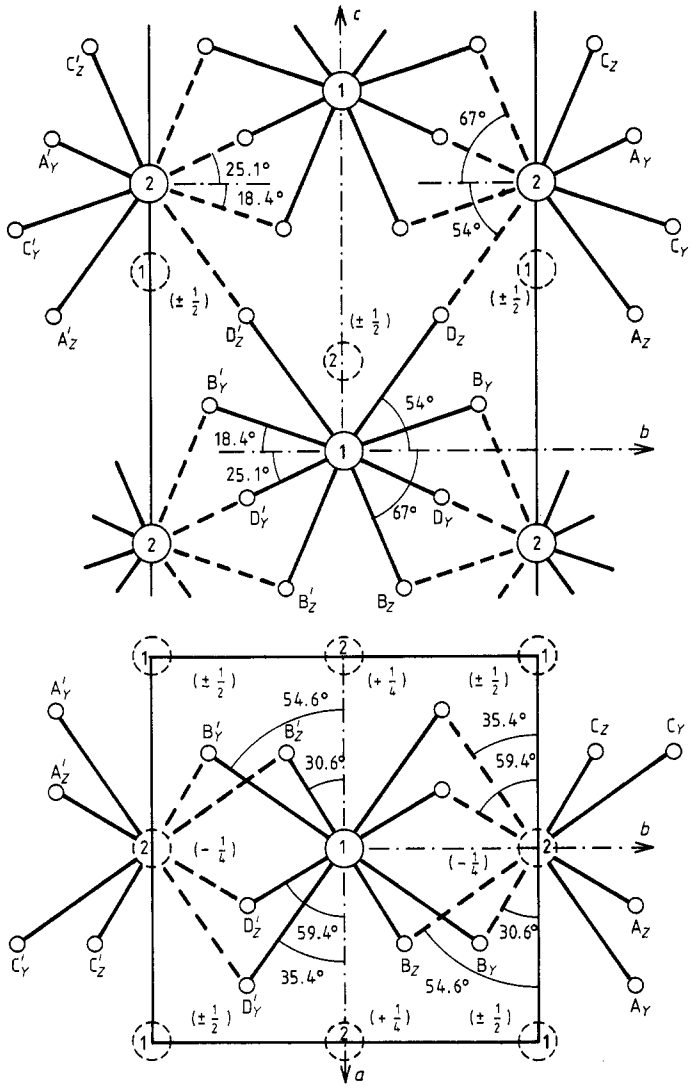

Figure 3. Projection of the KDP structure on the *a–b* and *b–c* planes. Here only the K^+ ions (large open circles) and H^+ ions (small open circles) are represented and the numbers 1 and 2 indicate the two different K sites. The directions of K^+–H^+ nearest-neighbour pairs are indicated by bold lines. These directions approximately coincide with the directions of the *Z* and *Y* axes of the eight defects A, A′, B, B′, C, C′, D and D′.

4. Discussion

To discuss the results presented in § 3, let us first consider the study in [12] on the EPR of Cr-doped KDP. As already mentioned, the EPR spectra and angular dependences for the resonance fields in [12] look rather similar to ours. This suggests we may be dealing with the same centre and that the observed differences could be attributed to some misorientation of either the sample used in [12] or our own growth band sample. However, it will be shown that this is not the case.

Table 1. Spin-Hamiltonian parameters and Eulerian angles for the eight sets of principal axes (see figure 3) for the defect associated with Cr^{3+} ions in the growth band region of KDP: $g_z = 1.972 \pm 0.001$; $g_y = 1.967 \pm 0.001$; $g_x = 1.972 \pm 0.004$; $B_2^0 = D/3 = 0.1457 \pm 0.0001\ cm^{-1}$; $B_2^2 = E = 0.1285 \pm 0.0001\ cm^{-1}$.

	K site 1				K site 2			
	B	B′	D	D′	A	A′	C	C′
θ_i (deg)	145.9	145.9	34.1	34.1	145.9	145.9	34.1	34.1
φ_i (deg)	16.8	196.8	106.8	286.8	73.2	253.2	163.2	343.2
ψ_i (deg)	240.7	240.7	299.3	299.3	119.3	119.3	60.7	60.7

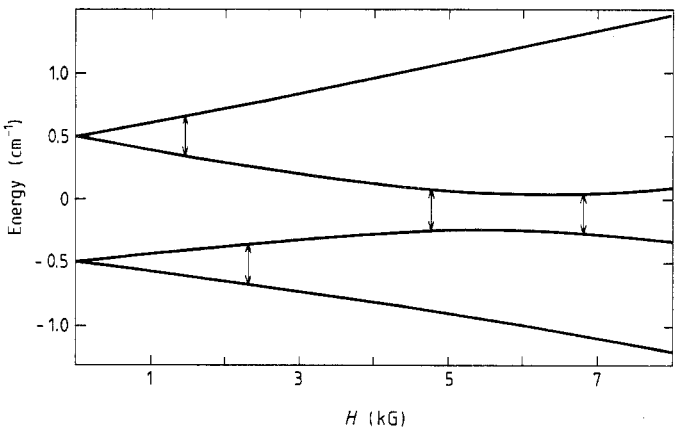

Figure 4. Energy levels of Cr^{3+} ions as a function of the magnetic field intensity for $\boldsymbol{H}$ parallel to the crystallographic c axis. The transitions are indicated by vertical arrows.

Our sample was carefully oriented, first by x-ray and subsequently inside the microwave cavity by using the EPR goniometer. This procedure gives good reproducibility in the angular dependences as shown in figure 2. In fact, any attempt to change the sample orientation slightly inside the microwave cavity results in splittings of most of the lines, indicating the high sensitivity on finding the right orientation. On the other hand, by using a regular sample (not the growth band region), the measured spectra as well as the angular variations coincide with those reported in [12]. Therefore it must be concluded that we are dealing with somehow similar although different defects.

The major experimental differences can be seen better by comparing figure 2(b) with the equivalent figure (figure 5) in [12]. The loop crossed by the ordinate corresponding to the c axis in figure 2(b), arising from the $|\frac{1}{2}\rangle \rightarrow |-\frac{1}{2}\rangle$ transition of A and D defects, is shifted towards the b axis in [12] (figure 5) so that the complete ellipse shape can be seen. This same transition for the other six defects has not been observed in [12], whereas it can readily be seen in figure 2(b). Also the curve for the $|\frac{3}{2}\rangle \rightarrow |\frac{1}{2}\rangle$ transition of A′ and D′ defects does not cross the loop in our case. It is difficult to compare our figure 2(a) showing the angular variation in the a–b plane with the corresponding figure (figure 9) in [12], since figure 9 in [12] is rather rough. The apparent differences, however, seem to be even larger for this figure.

The small differences exhibited by the spin-Hamiltonian parameters and principal axes obtained from the fitting are also significant. In our case the crystal-field strength is slightly smaller as indicated by slightly lower D- and E-values (table 1). The ratio $3E/D$, indicating the orthorhombic distortion strength, is also smaller in our sample. More significant is the fact that for Cr^{3+} in the growth band sample the Z axis, defined as the axis exhibiting maximum splitting, must be exchanged (within a few degrees) with the Y axis for Cr^{3+} in the bulk sample in [12].

As can be seen in figure 3, the Z axis for Cr^{3+} in the growth band sample approximately points to the position of a proton belonging to the so-called 'enlarged' proton tetrahedra (K^+–H^+ directions closer to that of the c axis), whereas the Y axis approximately points to the position of a proton belonging to the 'flattened' tetrahedra. This is contrary to the case for Cr^{3+} in [12]. As pointed out in [12], since the two axes with stronger crystal fields point to such proton positions, two proton vacancies (one from each tetrahedron) are the best candidates for local charge-compensating defects for Cr^{3+}. The exchange between Y and Z axes is an indication that the distortion of anion positions across the c axis for the growth band defect is greater than along the c axis, the contrary being true for the defect in [12].

This interpretation is further supported by the results reported in [11] on lattice parameter measurements of samples taken from the growth band region. By synchrotron radiation plane-wave reflection topography, an increase in the lattice parameter was found along the c axis in the growth band samples with respect to regular (inner) samples. This increase in the c parameter should induce a corresponding decrease in the crystal-field component along the c direction, as actually obtained in the present paper. Although the lattice parameters a and b have not been measured in [11], the exchange of Z and Y axes in the growth band sample suggests that a and b for these samples also have to be higher than for regular samples and that the distortion should be even higher than along the c axis.

References

[1] Müller K A 1974 *Ferroelectrics* **7** 17–21
[2] Adriaenssens G J 1977 *J. Magn. Reson.* **25** 511–7
[3] Müller K A 1987 *Ferroelectrics* **72** 273–304
[4] McMillan J A and Clemens J M 1978 *J. Chem. Phys.* **68** 3627–31
[5] Fujita I 1979 *J. Phys. Soc. Japan* **46** 1889–93
[6] Diéguez E and Cabrera J M 1981 *J. Phys. D: Appl. Phys.* **14** 91–7
[7] Diéguez E, Cabrera J M and Agulló-López F 1984 *J. Chem. Phys.* **81** 3369–74
[8] Diéguez E, Zaldo C, Cabrera J M and Agulló-López F 1985 *Induced Defects in Insulators* ed. P Mazzoldi pp 221–6
[9] Alybakov A A, Arbotoev O M, Gubanova V A and Kudabaev K 1985 *Phys. Status Solidi* b **128** K93–6
[10] Diéguez E, Cintas A, Hernández P and Cabrera J M 1985 *J. Cryst. Growth* **73** 193–5
[11] Belouet C, Dunia E, Pétroff J F and Sauvage M 1983 *J. Cryst. Growth* **61** 383–92
[12] Kobayashi T 1973 *J. Phys. Soc. Japan* **35** 558–72